PHYSICAL REVIEW D VOLUME 20, NUMBER 8 15 OCTOBER 1979

Analytic contributions to the g factor of the electron in sixth order

M. J. Levine
Carnegie-Mellon University, Pittsburgh, Pennsylvania 15213

E. Remiddi
Istituto di Fisica dell'Universita, Bologna, Italy
and Istituto Nazionale di Fisica Nucleare, Sezione di Bologna, Italy

R. Roskies
University of Pittsburgh, Pittsburgh, Pennsylvania 15260
(Received 4 June 1979)

We compute a precise value for three more graphs contributing to the g factor of the electron in sixth order. After comparing with other numerical and analytic evaluations, we give an updated "best" theoretical estimate of the g factor, and compare it to the experimental value.

I. INTRODUCTION

By combining the hyperspherical[1] and dispersive[2] techniques for Feynman-graph evaluation, we have computed the contributions of three more graphs to the g-factor anomaly of the electron in sixth order: $a_e^{(6)}$. These graphs are shown in Fig. 1. Recent high-precision experimental results[3] necessitate this continuing effort to improve the theoretical value for $a_e^{(6)}$. Our results are given in Table I. In Sec. II and in the Appendices we present details of the techniques used in this evaluation. In Sec. III we compare our results with previous, lower-precision, numerical results for these graphs and compare the overall theoretical results with recent high-precision experimental results for a_e.

II. TECHNIQUE

These results were obtained by a hybrid technique combining the hyperspherical approach used previously by two of the authors (M.L., R.R.) with the dispersion-theory methods already used by the third author (E.R.). Briefly, suitable subgraphs have been reduced to a dispersive representation. This representation is (a) relatively easily derived, (b) reduces the order of integration internal to the subgraph, and (c) is well suited to the remaining integrations needed to complete the evaluation. These remaining integrations are done by hyperspherical techniques. Below, we describe generally those techniques used in this field and, in particular, the combination used in this calculation.

The contribution of a given Feynman graph to the anomaly is usually first written in a form involving integrations over the virtual four momenta of the internal lines. In sixth-order QED this involves 3 four-fold integrations or 12 integrations. By introducing scalar "Feynman parameters" it is possible to reduce the order of integration from 12 to 7 or less. This is the technique used in the "numerical" work.[4-7] There the reduction to quadratures was done analytically.

The hyperspherical approach utilizes the fact that after performing the Wick rotation and introducing four-dimensional hyperspherical coordinates, it is often possible to do many or all of the angular integrations rather simply. These angular integrations are easy for some sixth-order graphs and become extremely difficult for other topologies. In the worst cases, we do not know how to apply this scheme at all. If the angular integrations can be done, then there remain the three "radial" integrals. These are of varying complexity. In simple cases, such as the ladder graph,[8] we encounter multiple simple rational functions which lead to logarithms and Spence functions after one or two integrations, respectively. In more complicated cases, we encounter higher-order generalized Spence or Nielsen[9] functions and the expressions involve square roots of rationals. A fuller discussion of these techniques can be found in Refs. 1 and 8.

Alternatively, one can work from dispersion-relation representations of the graphs. Following

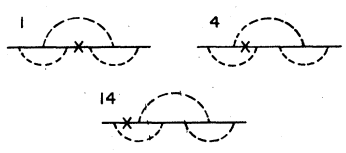

FIG. 1. Graphs evaluated in this paper. This is set F of Ref. 5. The numbering follows Ref. 4.

TABLE I. Quasianalytic expressions for the contribution to $a_e^{(6)}$ of the graphs in Fig. 1. The infrared pieces proportional to $\ln\lambda$ and $\ln^2\lambda$ are omitted. The values for graphs 4 and 14 have been doubled to include their mirror images. The numerical value is given as the sum of two parts: (1) an expression in the usual transcendental numbers and (2) a residual one-dimensionl integral.

Graph 1: $\frac{2929}{576}+\frac{431}{432}\pi^2-\frac{53}{216}\pi^4+\frac{2}{9}(\ln 2)^4+6\zeta(3)+\frac{16}{3}A_4-\frac{11}{9}\pi^2\ln 2+\frac{16}{9}\pi^2(\ln 2)^2+\frac{689}{96}\zeta(5)-\frac{383}{144}\pi^2\zeta(3)$

$+\int_0^1 db\,\mathrm{N1}=-22.9896\cdots+20.2383\cdots=-2.751\,419\,5$

Graph 4: $-\frac{7}{48}-\frac{295}{72}\pi^2-\frac{37}{432}\pi^4+\frac{1}{18}(\ln 2)^4+\frac{629}{12}\zeta(3)+\frac{4}{3}A_4+\frac{1}{3}\pi^2\ln 2+\frac{4}{9}\pi^2(\ln 2)^2-\frac{1153}{96}\zeta(5)-\frac{307}{48}\pi^2\zeta(3)$

$+\int_0^1 db\,\mathrm{N4}=-69.1612\cdots+67.9548\cdots=-1.206\,376\,5$

Graph 14: $+\frac{439}{144}+\frac{311}{144}\pi^2+\frac{\ }{1080}\pi^4-\frac{4}{9}(\ln 2)^4-\frac{1213}{24}\zeta(3)-\frac{32}{3}A_4-\frac{11}{18}\pi^2\ln 2-\frac{32}{9}\pi^2(\ln 2)^2-\frac{347}{96}\zeta(5)+\frac{539}{48}\pi^2\zeta(3)$

$+\int_0^1 db\,\mathrm{N14}=+108.5404\cdots-103.0304\cdots=+5.509\,933\,6$

Total: $+\frac{4601}{576}-\frac{203}{216}\pi^2+\frac{73}{720}\pi^4-\frac{1}{6}(\ln 2)^4+\frac{63}{8}\zeta(3)-4A_4-\frac{3}{2}\pi^2\ln 2-\frac{4}{3}\pi^2(\ln 2)^2-\frac{811}{96}\zeta(5)+\frac{313}{144}\pi^2\zeta(3)$

$+\int_0^1 db\,\mathrm{N_{tot}}=16.3895\cdots-14.8374\cdots=+1.552\,137\,6,$

where $\zeta(3)=\sum 1/(n^3)=1.202\,056\cdots$, $\zeta(5)=\sum 1/(n^5)=1.036\,927\cdots$, $A_4=\sum 1/(2^n n^4)=0.517\,479\cdots$

$\mathrm{N1}=\mathrm{I1}+19\times\mathrm{I2}+23\times\mathrm{I3}-5\times\mathrm{I4}$; $\mathrm{N4}=23\times\mathrm{I1}+29\times\mathrm{I2}+121\times\mathrm{I3}-523\times\mathrm{I4}$; $\mathrm{N14}=-23\times\mathrm{I1}-65\times\mathrm{I2}-157\times\mathrm{I3}+487\times\mathrm{I4}$

$\mathrm{N_{tot}}=\mathrm{I1}-17\times\mathrm{I2}-13\times\mathrm{I3}-41\times\mathrm{I4}$

$\mathrm{I1}=\mathrm{SMB\ LBM^2\ IB}+\mathrm{LGB}\ (2\ \mathrm{SB\ LB\ IBM}+3\ \mathrm{SMB\ LB\ IBM}+2\ \mathrm{LB\ LBM^2\ IB}+3\ \mathrm{LB\ LBM\ LB1\ IB}$

$-2\ \mathrm{SB\ LBM\ IB}-4\ \mathrm{SB\ LBM\ IBM}-3\ \mathrm{SMB\ LBM\ IB}-6\ \mathrm{SMB\ LBM\ IBM}-3\ \mathrm{LBM^2\ LB1\ IB})/3;$

$\mathrm{I2}=\mathrm{LGB}\ (4\ \mathrm{SB\ LB\ IB}+6\ \mathrm{SMB\ LB\ IB}-\mathrm{LBM^3\ IB}-3\ \mathrm{LB^2\ LB1\ IB})/12$; $\mathrm{I3}=\mathrm{LGB\ LB^3\ IB}/6$; $\mathrm{I4}=\mathrm{LGB\ LB^2\ LBM\ IB}/12$

and where $\mathrm{IB}=1/b$; $\mathrm{IBM}=1/(1-b)$; $\mathrm{LB}=\ln(b)$; $\mathrm{LBM}=\ln(1-b)$; $\mathrm{LB1}=\ln(1+b)$; $\mathrm{SB}=S_2(b)$; $\mathrm{SMB}=S_2(-b)$; $\mathrm{LGB}=\ln(1-b+b^2)$

Cutkosky[10] there are first the phase-space integrals to be evaluated in finding the discontinuity functions and finally the dispersion integral. The class of integrals encountered is the same as in the hyperspherical technique. Again there is a wide range of complexity among graphs. Because one deals with subgraphs on the mass shell in obtaining the discontinuities, there are a host of spurious infrared-divergence problems to be dealt with in this approach. These techniques are fully described in Ref. 2.

For the graphs of Fig. 1, the complexities of the angular integrals in a purely hyperspherical approach exceed our current personal and computer resources. If, however, we extract an off-mass-shell second-order vertex function from each graph and replace it by a dispersion integral form, the remaining angular integrals are nearly trivial. In the case of graph 1, it is even possible to extract both second-order vertex functions. In Appendix A we present the dispersive representation for the scalar second-order vertex function and derive it by hyperspherical techniques. This serves to demonstrate the basic analytical steps. In Appendix B we describe the additional steps necessary to derive the dispersive representation for the full spinor case. Using those functions one can write the amplitude for the full sixth-order graphs of Fig. 1 and extract the g-factor anomaly $a_e^{(6)}$. Since these are not new techniques, we omit further discussion of them.

At this stage one has seven dispersion integrals and some hyperspherical angular and one radial integral to evaluate. A sample term is considered in Appendix C where we describe the remaining steps in the integration. We are able to reduce the entire expression to a one-dimensional integral. Most of these integrals have been evaluated for previous graphs. Some new integrals of "transcendentality-4" (e.g., products of four logs and a rational or one Spence function, two logs and a rational) were encountered in these graphs. Appendix D is a table of some such integrals. Some new integrations were encountered which we are unable, as of yet, to do analytically. These have been given names and done to high precision (1

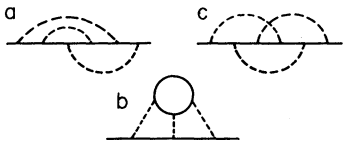

FIG. 2. Graphs not yet known to high precision. We show the basic self-energy graph from which the vertex graphs are derived by insertion of an external vertex.

part in 10^8) by numerical techniques.

III. RESULTS

In Table I we give the "semianalytic" results for each graph and its numerical contribution to a_e. While we are unable to evaluate all the integrals analytically, those integrals which remain are one dimensional and can be evaluated numerically to essentially arbitrary precision with reasonable ease. We present the remaining integrals in the form in which they arise in our calculation. But it is likely that only certain linear combinations of these simple forms arise and are reducible to our usual final class of transcendentals.

Our results are compared with results of previous numerical evaluations in Table II. The agreement with Ref. 4 is striking; the agreement with Refs. 5–7 is tolerable. The results of Carroll have usually been about one standard deviation more negative than the precise analytic results.

To obtain the best estimate of the total $a_e^{(6)}$, we combine those parts known analytically[1] and semianalytically with a weighted average of those with appreciable numerical errors. There are currently three sets of graphs in this latter category. The three sets are shown in Figs. 2(a)–2(c). The results for these sets from various sources are given in Table III and combined below (we treat the errors as statistical though they may well not be):

$$a_e^{(6)} = 1.181\,(10)\,.$$

Using this, $a_e^{(2)}$ (Ref. 11) and $a_e^{(4)}$ (Ref. 12) we obtain the current theoretical expression for the QED contribution:

$$a_e^{\rm th} = \tfrac{1}{2}(\alpha/\pi) - 0.328\,478\,445(\alpha/\pi)^2 + 1.181(10)(\alpha/\pi)^3\,. \tag{1}$$

The dominant unknown contribution to $a_e^{\rm th}$ is the eighth-order QED value which must be of order $(\alpha/\pi)^4 = 0.002(\alpha/\pi)^3$. Other known effects include fourth-order QED with muon loops (known exactly[13] $\sim 0.0002\ (\alpha/\pi)$,[3] fourth-order QED with hadronic loops[14] estimated to be $0.000\,13(2)(\alpha/\pi)^3$, and weak effects[15] which are estimated to be of order $0.000\,003(\alpha/\pi)^3$. These are presented here in units of $(\alpha/\pi)^3$ simply to demonstrate that they are still small compared to the uncertainties in $a_e^{(6)}$.

The relevant experimental numbers are the non-QED value[16] for the fine-structure constant

$$\alpha_{\rm NQED}^{-1} = 137.035\,963(15) \tag{2}$$

and the recent value for a_e from single trapped electrons by Van Dyck *et al.*,[3]

$$a_e^{\rm exp} = 1\,159\,652\,200\,(40) \times 10^{-12}\,. \tag{3}$$

We can combine (1) and (2) to yield

$$a_e^{\rm th} = 1\,159\,652\,541(179) \times 10^{-12}\,. \tag{4}$$

This error comes from uncertainties in α, 127×10^{-12}, and in a_e^6, 125×10^{-12}. Alternatively we can combine (1) and (3) to yield

$$\alpha^{-1} = 137.036\,003\ (16)\,. \tag{5}$$

This error comes from uncertainties in $a_e^{\rm exp}$, 5×10^{-6}, and in $a_e^{\rm th}$, 15×10^{-6}. Comparing (4) with (3) and (5) with (2) both give reasonable agreement.

TABLE II. Comparison between the results of this paper and previous results for these graphs. Values for nonsymmetric graphs have been doubled.

Graph	Results from this paper	Previous results		
1	−2.751 919 5	−2.746 (7)[a]	−2.733 (6)[b]	−2.728 (16)[d]
4	−1.206 376 5	−1.211 (13)[a]	−1.200 (7)[b]	
14	+5.509 933 6	5.515 (25)[a]	5.488 (14)[b]	
Total	+1.552 137 6	1.559 (29)[a]	1.551 (10)[b]	1.532 (15)[c]

[a] Reference 4.
[b] References 5 and 20.
[c] Reference 6.
[d] Reference 7.

TABLE III. Numerical values for the graphs of Fig. 2. These are not yet known to high precision.

	Graphs of Fig. 2(a)	2(b)	2(c)
Values from other sources	0.0893 (60) [a]	0.3600 (400) [d]	0.7807 (13) [h]
	0.0970 (280) [b]	0.3660 (100) [e]	0.7980 (240) [b]
	0.0470 (300) [c]	0.3700 (130) [f]	0.7730 (140) [c]
		0.4000 (40) [g]	
Value used in this paper	0.0897 (58)	0.3680 (80)	0.7807 (13)

[a] Reference 20.
[b] Reference 4.
[c] Reference 6.
[d] Reference 21.
[e] Reference 22.
[f] Reference 23.
[g] Reference 24.
[h] Reference 17.

Work continues both on a_e^{exp} and on the remaining numerical parts of $a_e^{(6)}$. Our techniques are being applied to produce high-precision results for the graphs of Figs. 2(a), and (b). As yet, we do not understand how to approach the nonplanar graphs of Fig. 2(c). The recent numerical reevaluation of this set by Kinoshita and Lindquist[17] has reduced the error due to this set to the same order of magnitude as our uncertainty in the eighth-order QED effects. Because of continuing experimental work, it will probably become necessary finally to come to grips with $a_e^{(8)}$.

ACKNOWLEDGMENTS

The work of M.J.L. was supported in part by the U.S. Department of Energy. The work of R.R. was supported in part by the U.S. National Science Foundation.

APPENDIX A

We show here how to obtain the dispersive representation of the second-order scalar vertex graph by means of hyperspherical integration. This method can be useful because it gives directly any necessary subtraction terms in the dispersive representation. Additionally, it provides a simple, explicit example of the hyperspherical technique.

The scalar vertex amplitude, corresponding to the graph in Fig. 3, is

$$V(Q^2,P^2,L^2)=\frac{i}{(2\pi)^2}\int d^4k\,D^{-1},$$
$$D=(k^2+1)(P-k)^2[(L-k)^2+1], \tag{A1}$$

where k is the Minkowski loop momentum. We have set $m_e=1$. We use the metric $P^2=\vec{P}^2-P_0^2$. The Q^2 dispersion relation at fixed P^2, L^2 for this amplitude is

$$V(Q^2,P^2,L^2)=\frac{1}{\pi}\int_1^\infty \frac{da}{(a+Q^2)}\,v(a,-P^2,L^2). \tag{A2}$$

For $L^2>0$ (spacelike) and $P^2\to -1$ (mass-shell condition) the discontinuity is

$$v(a,1,L^2)=-\frac{1}{4}\frac{1}{R_a}\ln[(a+1+L^2+R_a)/(a+1+L^2-R_a)], \tag{A3}$$

where the characteristic root is

$$R_a=[(a-1+L^2)^2+4L^2]^{1/2}.$$

This expression for the discontinuity can be readily obtained by the Cutkosky rules.[10]

Alternatively, we can evaluate most of the integrals in (A1) by hyperspherical techniques to rederive the dispersive representation. For $L^2>0$, P^2 real and >-1 we can Wick rotate k into the Euclidean momentum K. Then

$$d^4k=d^3k\,dk_0\to i\,d^3K\,dK_0=i\,d^4K=i\,K^3\,dK\,d^3\Omega(\hat{K}).$$

K is the "radial" variable ($0\leq K<\infty$) and $d^3\Omega(\hat{K})$ refers to the three hyperspherical angles. The Gegenbauer polynomials $C_n(w)$ enter naturally. We need their generating function

$$1/(z^2-2wz+1)=\sum_{n=0}^{\infty} z^n C_n(w), \tag{A4}$$

orthogonality condition

$$\int d^3\Omega(\hat{K})C_n(\hat{P}\cdot\hat{K})C_m(\hat{K}\cdot\hat{Q})=2\pi^2\frac{\delta_{nm}}{(n+1)}C_n(\hat{P}\cdot\hat{Q}) \tag{A5}$$

(where $\hat{P}\cdot K$ is the cosine of the angle between the four-dimensional vectors P and K), addition theorem

$$C_n(x)C_m(x)=\sum_{j=0}^{\text{Min}(n,m)} C_{m+n-2j}(x), \tag{A6}$$

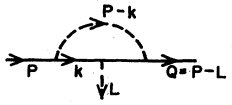

FIG. 3. The second-order scalar vertex graph.

and special cases $C_0(x)=1$, $C_1(x)=2x$. The generating function is essentially the Euclidean scalar propagator so that

$$1/[(K-L)^2+m^2]=\frac{z}{(KL)}\sum_{n=0}^{\infty} z^n C_n(\hat{K}\cdot\hat{L}), \qquad \text{(A7)}$$

where

$$z=z(K,L,m^2)$$
$$=\{(K^2+L^2+m^2)$$
$$-[(K^2+L^2+m^2)^2-4K^2L^2]^{1/2}\}/(2KL).$$

Since we sometimes encounter squared propagators, we might also require that

$$1/[(K-L)^2+m^2]^2$$
$$=\frac{z^2}{[(KL)^2(1-z^2)]}\sum_{n=0}^{\infty}(n+1)z^n C_n(\hat{K}\cdot\hat{L}), \qquad \text{(A8)}$$

obtained by differentiating (A7) with respect to m^2.

Considering those parts of (A1) depending upon the direction of K, we define

$$I=\int\frac{d^3\Omega(K)}{(P-K)^2[(L-K)^2+1]}.$$

Using (A7) we have

$$I=\int d^3\Omega(K)\frac{xy}{(PLK^2)}\sum_{n,m=0}^{\infty}x^n y^m C_n(\hat{P}\cdot\hat{K})C_m(\hat{K}\cdot\hat{L}).$$

x is the $z(K,L,1)$ of (A7), y is $z(P,K,0)$ and depends upon the magnitude of P/K:

$$y=P/K \text{ if } P<K$$
$$=K/P \text{ if } P>K.$$

Application of (A5) yields

$$I=\frac{2\pi^2}{(PLK^2)}\sum_{n=0}^{\infty}\frac{(xy)^{n+1}}{(n+1)}C_n(\hat{P}\cdot\hat{L}).$$

Integrating (A4) with respect to z allows us to write

$$I=\frac{2\pi^2}{(PLK^2)}\int_0^{xy}dw/(w^2-2\hat{P}\cdot\hat{L}\,w+1). \qquad \text{(A9)}$$

Using (A9) in (A1) yields

$$V(Q^2,P^2,L^2)$$
$$=-\frac{1}{(2PL)}\int_0^{\infty}\frac{KdK}{(K^2+1)}\int_0^{xy}\frac{dw}{(w^2-2\hat{P}\cdot\hat{L}\,w+1)}.$$

Interchanging orders of integration and limits, we have

$$V(Q^2,P^2,L^2)=-\frac{1}{(4PL)}\int_0^{z_w}\frac{dw}{(w^2-2P\cdot L\,w+1)}$$
$$\times\int_{K_-^2}^{K_+^2}\frac{dK^2}{K^2+1},$$

where

$$z_w=z(P,L,1),$$
$$K_+=P\frac{(L^2+1)z-PL}{z(zL-P)},$$
$$K_-=zP\frac{(L^2+1)-PLz}{(L-Pz)}.$$

The K^2 integration is now trivial. If we now replace w by the variable a defined implicitly by

$$w=z(P,L,a)$$

we recover the dispersive representation. The limit $P^2\to -1$ is readily taken to reproduce (A3).

APPENDIX B

The introduction of spin and the taking of the P leg of Fig. 3 slightly off-mass-shell broadens the required class of second-order vertex integrals beyond that given in (A2), (A4). Here we describe the derivation of this set of functions. The method is of utility in other graphs contributing to $a_e^{(6)}$. The second-order spinor vertex requires that we consider not simply

$$V=\frac{i}{(2\pi)^2}\int d^4k\,D^{-1},$$
$$D=(k^2+1)(P-k)^2[(L-k)^2+1],$$

as in (A1) but rather the set

$$[V;U_\alpha;T_{\alpha\beta}]=\frac{i}{(2\pi)^2}\int d^4k\,D^{-1}[1;k_\alpha;k_\alpha k_\beta]. \qquad \text{(B1)}$$

The full second-order vertex involves combinations of these functions with L_μ and various Dirac matrices. Since it is usual and straightforward, we do not present it here.

In analogy with (A2) the results can be written as (in particular, see p. 912 of Ref. 25)

$$[V;U_\alpha;T_{\alpha\beta}]=\frac{1}{\pi}\int^{\infty}\frac{da}{(a+Q^2)}[v;u_\alpha;t_{\alpha\beta}], \qquad \text{(B2)}$$

where v, u, t depend upon the vectors P_α and L_α and the invariants (a,P^2,L^2). Lorentz covariance limits the form of u_α and $t_{\alpha\beta}$ to

$$u_\beta=u_1P_\alpha+u_2L_\alpha,$$
$$t_{\alpha\beta}=t_1g_{\alpha\beta}+t_2P_\alpha P_\beta+t_3L_\alpha L_\beta+t_4(P_\alpha L_\beta+L_\alpha P_\beta), \qquad \text{(B3)}$$

where $u_{1,2}$ and $t_{1,2,3,4}$ are scalar discontinuity functions. The absence of kinematical singularities in the Q^2-dispersion relation for the u's and t's means that in deriving the discontinuity functions one can replace $Q^2=(P-L)^2$ by $-a$ everywhere in v,u,t, thereby leaving the explicit $(a+Q^2)^{-1}$ as the only dependence upon the angle be-

tween L and P. Explicit expressions can be obtained for these discontinuities $u_{1,2}$ ($t_{1\text{-}4}$) by the use of a complete, orthonormal set of vectors (tensors) spanning the appropriate space.

We introduce two orthonormal vectors r_α, s_α. One possible choice is

$$r_\alpha = bP_\alpha, \quad s_\alpha = c(L_\alpha - bL\cdot P\, r_\alpha), \tag{B4}$$

with b,c such that $r\cdot r = s\cdot s = 1$, $r\cdot s = 0$: $b^{-2} = P\cdot P$, $c^{-2} = L^2 - (L^2+P^2+a)^2/(4P^2)$. We have replaced $(L-P)^2$ by $-a$. Using the completeness of r and s in the space spanned by L and P, we can then rewrite the k_α of (B1) as

$$k_\alpha = (r_\alpha r_\beta + s_\alpha s_\beta)k_\beta = r_\alpha(r\cdot k) + s_\alpha(s\cdot k) \tag{B5}$$

so that the free index no longer appears on the variable of integration k. In deriving the discontinuity functions u_1 and u_2 we must now extract the coefficients of P_α and L_α from (B5), replace all dependence upon $P\cdot L$ or Q^2 with appropriate functions of a, and, in general, follow the procedures of Appendix A or the Cutkosky rules in producing the discontinuities $u_{1,2}$.

Similarly, we can obtain $t_{1\text{-}4}$ using the complete, orthonormal tensors

$$\tau_{1\alpha\beta} = r_\alpha r_\beta,$$
$$\tau_{2\alpha\beta} = s_\alpha s_\beta,$$
$$\tau_{3\alpha\beta} = (r_\alpha S_\beta + S_\alpha r_\beta)/\sqrt{2},$$
$$\tau_{4\alpha\beta} = (\delta_{\alpha\beta} - \tau_{1\alpha\beta} - \tau_{2\alpha\beta})/\sqrt{2}$$

and the replacement

$$k_\alpha k_\beta = \sum_{i=1}^{4} (\tau_{i\alpha\beta}\tau_{i\mu\nu})k_\mu k_\nu .$$

While the algebraic work involved is not prohibitive by hand, we did it by machine using ASHMEDAI.[18]

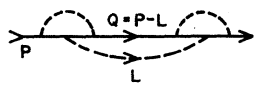

FIG. 4. The scalar self-energy graph corresponding to the vertex graphs of Fig. 1.

To extract the contribution of the sixth-order graphs to $a_e^{(6)}$ we need more than the $[V;U_\alpha;T_{\alpha\beta}]$ of (B2) for P_α on the mass shell. In addition, we need the first-order terms of V,U,T as functions of $(P+q/2)$ in the limit that q_α, the external photon momentum, goes to zero. The terms arise in two ways. First, we must replace the explicit P_μ of (B3) with $(P_\mu + q_\mu/2)$. Second, we consider the q dependence of Q^2 in (B2). Thus for V we need

$$V \to V|_{q=0} + \left.\frac{\partial V}{\partial P_\mu}\right|_{q=0} \frac{q_\mu}{2}$$

but

$$\frac{q_\mu}{2}\frac{\partial V(P^2,L^2,L\cdot P)}{\partial P_\mu} = \frac{q_\mu}{2}\left(\frac{\partial V}{\partial P^2}2P_\mu + \frac{\partial V}{\partial(L\cdot P)}L_\mu\right)$$
$$= -(q\cdot L)\left.\frac{\partial V}{\partial Q^2}\right|_{q=0}$$
$$= +(q\cdot L)\int_1^\infty \frac{da}{(a+Q^2)^2}\, v(P^2,L^2,a)$$

since $q\cdot P = 0$.

Thus for each of the discontinuities of (B3) we get an additional one obtained by multiplying by $(q\cdot L)/(a+Q^2)$.

Some of the expressions (e.g., t_1) are divergent: the result of ultraviolet divergences in the second-order vertex. As long as we carry the proper renormalization counterterm through the same formal manipulation as the main second-order graph, the difference is both finite and correct.

APPENDIX C

To give an idea of the analytic underlying structure of the calculation, we sketch here our approach to a typical term, corresponding to the scalar self-mass amplitude of Fig. 4. Using (A2) and (A3) for the inserted vertex parts, disregarding numerical factors, and using hyperspherical L-loop variables for $P^2 = -1$, we define

$$X \equiv \frac{2}{\pi^2}\int_0^\infty \frac{L^3dL}{L^2}\int \frac{d\Omega(\hat{L})}{(P-L)^2+1}\int_1^\infty \frac{db}{b+(P-L)^2}\frac{1}{R_b}LR(b)\int_1^\infty \frac{da}{a+(P-L)^2}\frac{1}{R_a}LR(a), \tag{C1}$$

where

$$R_b = R(b) = [(b-1+L^2)^2+4L^2]^{1/2}, \quad R_a = R(a), \quad LR(a) = \ln[(a+1+L^2+R(a))/(a+1+L^2-R(a))].$$

We use partial fractions for all denominators in $(P-L)^2$ and use

$$\int \frac{d\Omega(L)}{(K-L)^2+C} = 2\pi^2\{K^2+L^2+C-[(K^2+L^2+C)-4K^2L^2]^{1/2}\}/(2K^2L^2). \tag{C2}$$

TABLE IV. Integrals of transcendentality-4. The first column is the integrand. This is to be integrated in t from 0 to 1. The next eight columns give the rational coefficients for the eight transcendental constants: $C_1=\zeta(5)$, $C_2=\zeta(2)\zeta(3)$, $C_3=A_5$, $C_4=A_4\ln 2$, $C_5=\zeta^2(2)\ln 2$, $C_6=\zeta(3)\ln^2 2$, $C_7=\zeta(2)\ln^3 2$, $C_8=\ln^5 2$, where $A_5=\sum 1/(2^n n^5)$. The Nielsen functions are defined in Ref. 9.

Integrand	C_1	C_2	C_3	C_4	C_5	C_6	C_7	C_8
$\ln t\ln^3(1-t)/t$	12	−6						
$\ln^4(1+t)/t$	24		−24	−24		$-\frac{21}{2}$	4	$-\frac{4}{5}$
$\ln t\ln^3(1+t)/t$	$+\frac{99}{64}$	3	−12	−12		$-\frac{21}{4}$	2	$-\frac{2}{5}$
$\ln^2 t\ln^2(1+t)/t$	$-\frac{29}{8}$	2						
$\ln^3 t\ln(1+t)/t$	$-\frac{45}{8}$							
$\ln^4(1-t/2)/t$	24		−24	−24		$-\frac{21}{2}$	4	−1
$\ln t\ln^3(1-t/2)/t$	$\frac{189}{16}$	−3	−6		$-\frac{12}{5}$	$\frac{21}{8}$	$-\frac{1}{2}$	$\frac{1}{10}$
$\ln^2 t\ln^2(1-t/2)/t$	$\frac{1}{8}$	−2	4	4	$-\frac{1}{5}$	2	$-\frac{2}{3}$	$\frac{1}{10}$
$\ln^2 t\ln^2(1-t)/t$	8	−4						
$\ln^3 t\ln(1-t)/(1+t)$	$\frac{273}{16}$	$-\frac{9}{2}$			$-\frac{9}{2}$			
$\ln^2 t\ln(1-t)\ln(1+t)/t$	$-\frac{27}{16}$	$\frac{3}{4}$						
$\ln^3 t\ln(1+t)/(1-t)$	12	$-\frac{9}{4}$			$-\frac{9}{2}$			
$\ln^3 t\ln(1+t)/(1+t)$	$\frac{87}{16}$	−3						
$\ln t\ln(1-t)\ln^2(1+t)/t$	$-\frac{25}{16}$	$\frac{7}{8}$						
$\ln t\ln^2(1-t)\ln(1+t)/t$	$-\frac{7}{2}$	$-\frac{3}{8}$	4	4		$\frac{7}{4}$	$-\frac{2}{3}$	$\frac{2}{15}$
$\ln^3(1-t)\ln t/(1+t)$	$-\frac{3}{16}$	$-\frac{21}{4}$	18		$\frac{9}{10}$			$-\frac{3}{20}$
$\ln^4 t/(1+t)$	$\frac{45}{2}$							
$\ln^4(1-t)/(1+t)$			24					
$\ln^2 t\ln^2(1-t)/(1+t)$	$\frac{15}{2}$	$-\frac{13}{2}$	8		$\frac{2}{5}$		$\frac{2}{3}$	$-\frac{1}{15}$
$\ln(1+t)S_3(t)/t$	$\frac{59}{32}$	$-\frac{3}{4}$						
$\ln t\ln(1+t)S_2(t)/t$	$\frac{107}{32}$	$-\frac{15}{8}$						
$\ln t\,S_3(t)/(1+t)$	$-\frac{83}{16}$	$\frac{21}{8}$						
$\ln^2 t\,S_2(t)/(1+t)$	$-\frac{67}{8}$	$\frac{9}{2}$						
$S_2(t)S_2(-t)/t$	$\frac{59}{32}$	$\frac{5}{4}$						
$\ln t\ln(1-t)S_2(-t)/t$	$-\frac{3}{2}$	$\frac{5}{8}$						
$\ln^2 t\,S_2(-t)/(1-t)$	$-\frac{21}{16}$	$\frac{1}{2}$						
$\ln t\ln^3[(1-t)/(1+t)]/t$	$\frac{93}{8}$	$-\frac{21}{4}$						
$\ln t\ln^3(1-t^2)/t$	3	$-\frac{3}{2}$						
$S_4(-t)/(1+t)\,dt$	$\frac{17}{16}$	$-\frac{3}{8}$			$-\frac{7}{20}$			
$\ln(1+t)S_3(-t)/t$	$-\frac{17}{16}$	$\frac{3}{8}$						
$S_2{}^2(-t)/t$	$-\frac{17}{16}$	$\frac{3}{4}$						
$\ln t\ln(1+t)S_2(-t)/t$	$-\frac{17}{32}$	$\frac{3}{8}$						
$\ln^2 t\,S_2(-t)/(1+t)$	$-\frac{41}{16}$	$\frac{5}{4}$						
$\ln t\,S_3(-t)/(1+t)$	$\frac{51}{32}$	$-\frac{3}{4}$						
$\ln(1-t)S_3(t)/(1+t)$	$-\frac{85}{16}$	2	2		$\frac{1}{10}$	$-\frac{3}{8}$	$\frac{1}{6}$	$-\frac{1}{60}$
$\ln(1-t)S_3(t)/t$	−3	1						
$\ln t\ln(1-t)S_2(t)/t$	$-\frac{3}{2}$	1						
$\ln t\,S_3(t)/(t-1)$	$\frac{9}{2}$	−2						
$\ln^2 t\,S_2(t)/(t-1)$	11	−6						

TABLE IV. (*Continued*)

Integrand	C_1	C_2	C_3	C_4	C_5	C_6	C_7	C_8
$\ln^2(1-t)S_2(t)/t$	-1	2						
$\ln(1-t)S_{1,2}(t)/t$	$-\frac{1}{2}$							
$[S_2^2(t)-S_2^2(1)]/(t-1)$	-2	4						
$\ln^2(1-t)\ln^2(1+t)/t$	$-\frac{25}{8}$		4	4		$\frac{7}{4}$	$-\frac{2}{3}$	$\frac{2}{15}$
$\ln(1-t)\ln^3(1+t)/t$	$\frac{3}{4}$	$\frac{21}{8}$	-6	-6		$-\frac{21}{8}$	1	$-\frac{1}{5}$
$\ln^3(1-t)\ln(1+t)/t$	$-\frac{31}{16}$	$-\frac{21}{8}$	6	6		$\frac{21}{8}$	-1	$\frac{1}{5}$
$\ln^2(1+t)S_2(t)/(1+t)$	$\frac{1}{4}$	$\frac{7}{8}$	-2	-2		$-\frac{7}{8}$	$\frac{2}{3}$	$-\frac{1}{15}$
$\ln t\ln^2(1-t)\ln(1+t)/(t-1)$	$\frac{7}{4}$	$\frac{21}{8}$	-8	-2	$-\frac{3}{10}$	$-\frac{7}{8}$	$\frac{1}{3}$	$-\frac{1}{60}$
$\ln^4(1-t)/t$	24							
$\ln(1-t)\ln^3 t/t$	6							

We get

$$X=\int_0^\infty \frac{dL^2}{[L^2(L^2+4)]^{1/2}}\frac{1}{L^2}F(L^2)$$
$$=-\frac{1}{2}\left(\frac{L^2+4}{L^2}\right)^{1/2}F(L^2)\Big|_0^\infty$$
$$+\tfrac{1}{2}\int_0^\infty dL^2\left(\frac{L^2+4}{L^2}\right)^{1/2}\frac{dF}{dL^2}\,, \qquad \text{(C3)}$$

where the second expression for X in (C3) is obtained by integrating by parts, and

$$F(L^2)=[L^2(L^2+4)]^{1/2}\int_1^\infty \frac{db}{b-1}\frac{1}{R_b}LR(b)H(b,L^2)\,, \qquad \text{(C4)}$$

$$H(b,L^2)=\int_1^\infty da\left[\left(1-\frac{R_b}{R_a}\right)\frac{1}{a-b}\right.$$
$$\left.-\left(1-\frac{[L^2(L^2+4)]}{R_a}\right)^{1/2}\frac{1}{a-1}\right]LR(a)\,. \qquad \text{(C5)}$$

Explicit integration of (C5) is possible by using, for instance, the integration variable

$$y=\frac{R_a-a-L^2+1}{2}$$

The explicit result, however, is an unmanageable sum of dilogarithms and products of two logarithms (transcendentality-2 functions) of complicated arguments which is of little use for subsequent b, L^2 integrations.

It is more convenient to use the integral representation (C5) for evaluating b and L^2 derivatives of $H(b,L^2)$, as well as its end-point values at $b=1,\infty$, and $L^2=0,\infty$. These derivatives of H will be used to find the corresponding derivatives of F which will be used in the second expression for X of (C3).

After some algebra and integration by parts in a, along the lines of Sec. 5.1 of Ref. 19, the a integrand involves rational functions only, which are integrated to give combinations of logarithms. The expressions for $\partial H/\partial L^2$ and $\partial H/\partial b$ are cumbersome but manageable.

As a next step, we consider the transcendentality-3 functions, as for instance

$$G(L^2)=\int_1^\infty db\left(\frac{1}{b-1}-\frac{1}{b}\right)H(b,L^2)\,, \qquad \text{(C6)}$$

whose integral representations involve transcendentality-2 functions. Its L^2 derivative involves $\partial H/\partial L^2$ only, previously evaluated, and the b-integration can be done explicitly. Because $G(L^2)$ and so $dG(L^2)/dL^2$ depend only on L^2, from the explicit knowledge of dG/dL^2 it is not too difficult to also obtain $G(L^2)$. When use is made of the variable

$$t=\frac{L^2+2-[L^2(L^2+4)]^{1/2}}{2}$$

the result is found to consist of combinations of Nielsen functions and logarithms of relatively simple arguments. We then deal similarly with $F(L^2)$ of Eq. (C4) which is of transcendentality-4. Owing to the factor $[L^2(L^2+4)]^{1/2}$ in the definition, its L^2 derivative is a combination of transcendentality-3 functions, such as $G(L^2)$. dF/dL^2 and the value of $F(L^2)$ for $L^2\to 0$ are sufficient for obtaining X, Eq. (C1), after an integration by parts, as a definite single integral of an explicitly known function.

In the actual calculation of the whole $g-2$ contribution, after using the dispersive representations for the two inserted one-loop vertices, one has, instead of (C1), an integral over the same varia-

bles involving, however, some thousand terms, roughly consisting of the same factors occurring in (C1) to a variety of different powers. The algebraic work was done by computer.[18] At any step we try to perform as many as possible integrations by parts, to reduce the size of the expression, and then proceed as above. A total of about two dozen functions of various transcendentalities suffices. There is the usual blowing up of the number of terms in intermediate steps, but the last t integrand is relatively simple, a few hundred terms.

All final definite single integrals involving transcendentality-3 functions were known and done analytically, so giving at most transcendentality-4 constants. In addition, in the class of graphs we considered, for the first time in analytic $(g-2)$ calculations there are terms involving transcendentality-4 functions which presumably give transcendentality-5 constants, such as $\zeta(5)$, $\zeta(2)\zeta(3)$, etc. So far, we have succeeded in analytically evaluating only a subset of them. The numerical integration of the remaining terms is simple enough (definite integral between 0 and 1 of an explicitly known function, with end-point logarithmic singularities only) to be carried out without any trouble to almost arbitrary precision.

APPENDIX D

We present here a collection of one-dimensional integrals of fourth-order integrands. This is an extension of the third-order table in Ref. 25. The order is based on the Nielsen function: ln, $S_2, \ldots$ contribute $1, 2, \ldots$ to the order. Thus these integrands contain four logarithms or two logarithms + one Spence function, etc. The table is not exhaustive. We have not used all of the integrals in this calculation. However, since this family of integrals is likely to arise in any approach to these graphs and since different approaches may require different members of the set, we present what we have. Table IV contains the integrals. The method of derivation is the same as for the third-order table. We thank Michele Caffo for some entries.

[1]M. J. Levine and R. Roskies, Phys. Rev. D 14, 2191 (1976) and references therein.

[2]R. Barbieri, M. Caffo, and E. Remiddi, Phys. Lett. 57B, 460 (1975), Ref. 19 of this paper and references therein.

[3]R. S. Van Dyck, Jr., P. B. Schwinberg, and H. G. Dehmelt, Bull. Am. Phys. Soc. 24, 758 (1979).

[4]M. J. Levine and J. Wright, Phys. Rev. D 8, 3171 (1973).

[5]P. Cvitanović and T. Kinoshita, Phys. Rev. D 10, 4007 (1974).

[6]R. Carroll, Phys. Rev. D 12, 2344 (1975).

[7]A. De Rujula, B. Lautrup, and A. Peterman, Phys. Lett. 33B, 605 (1970).

[8]M. J. Levine and R. Roskies, Phys. Rev. D 9, 421 (1974).

[9]L. Lewin, *Dilogarithms and Associated Functions* (MacDonald, London, 1958); K. S. Kölbig, J. A. Mignaco, and E. Remiddi, BIT 10, 38 (1970); R. C. Perisho, U. S. AEC Report No. COO-3066-45, 1975 (unpublished); N. Nielsen, Nova Acta, Abh. d. Kaiserl. Leop.-Carol. Deutschen Akademie d. Naturforscher 90, 123 (1909).

[10]R. E. Cutkosky, J. Math. Phys. 1, 429 (1960).

[11]J. Schwinger, Phys. Rev. 73, 416 (1948).

[12]R. Karplus and N. M. Kroll, Phys. Rev. 77, 536 (1950). Errors in this paper were corrected in A. Peterman, Helv. Phys. Acta 30, 407 (1957); C. M. Sommerfield, Ann. Phys. (N.Y.) 5, 26 (1958); M. V. Terent'ev, Zh. Eksp. Teor. Fiz. 43, 619 (1962) [Sov. Phys.—JETP 16, 444 (1963)].

[13]B. E. Lautrup and E. de Rafael, Phys. Rev. 174, 1835 (1968).

[14]This estimate is obtained by multiplying the corresponding quantity for the muon moment given by J. Calmet *et al.*, Rev. Mod. Phys. 49, 21 (1977), by $(m_e/m_\mu)^2$.

[15]R. Jackiw and S. Weinberg, Phys. Rev. D 5, 2473 (1972); I. Bars and M. Yoshimura, *ibid.* 6, 374 (1972); W. A. Bardeen, R. Gastmans, and B. E. Lautrup, Nucl. Phys. B46, 319 (1972).

[16]E. R. Williams and P. T. Olsen, Phys. Rev. Lett. 42, 1575 (1979).

[17]T. Kinoshita and B. Lindquist, Cornell Report No. CLNS-374, 1977 (unpublished).

[18]M. J. Levine, U.S. AEC Report No. CAR-882-25, 1971 (unpublished). See also M. J. Levine, in Proceedings of the Third International Colloquium in Advanced Computing Methods in Theoretical Physics, Marseille, 1973, edited by A. Visconti (unpublished), and R. C. Perisho, ASHMEDAI User's Guide, U.S. AEC Report No. COO-3066-44, 1975 (unpublished).

[19]R. Barbieri and E. Remiddi, Nucl. Phys. B90, 233 (1975).

[20]P. Cvitanović and T. Kinoshita, private communication.

[21]J. Aldins, S. J. Brodsky, A. Dufner, and T. Kinoshita, Phys. Rev. D 1, 2378 (1970).

[22]J. Calmet and A. Peterman, Phys. Lett. 47B, 369 (1973).

[23]C. T. Chang and M. J. Levine, 1973 (unpublished).

[24]M. A. Samuel and C. Chlouber, Phys. Rev. D 18, 613 (1978).

[25]R. Barbieri, J. A. Mignaco, and E. Remiddi, Nuovo Cimento A11, 824 (1972).